




Article

Changes in the Chemical Composition of Polyethylene Terephthalate under UV Radiation in Various Environmental Conditions

Sara Rostampour^{1,2,*}, Rachel Cook³, Song-Syun Jhang⁴, Yuejin Li², Chunlei Fan² and Li-Piin Sung^{3,*}

¹ PREP Associate, Infrastructure Materials Group, Materials and Structural Systems Division, National Institute of Standards and Technology, Gaithersburg, MD 20899, USA

² Bio Environmental Science Program, Morgan State University, Baltimore, MD 21251, USA; yuejin.li@morgan.edu (Y.L.); chunlei.fan@morgan.edu (C.F.)

³ Infrastructure Materials Group, Materials and Structural Systems Division, National Institute of Standards and Technology, Gaithersburg, MD 20899, USA; rachelelizabetchcook@gmail.com

⁴ Department of Materials Science and Engineering, National Cheng Kung University, No. 1, University Rd., Tainan 701, Taiwan; zx55kk55aa@gmail.com

* Correspondence: sara.rostampour5@gmail.com (S.R.); li-piin.sung@nist.gov (L.-P.S.)

Abstract: Polyethylene terephthalate has been widely used in the packaging industry. Degraded PET micro(nano)plastics could pose public health concerns following release into various environments. This study focuses on PET degradation under ultraviolet radiation using the NIST SPHERE facility at the National Institute of Standards and Technology in saturated humidity (i.e., $\geq 95\%$ relative humidity) and dry conditions (i.e., $\leq 5\%$ relative humidity) with varying temperatures (30 °C, 40 °C, and 50 °C) for up to 20 days. ATR-FTIR was used to characterize the chemical composition change of degraded PET as a function of UV exposure time. The results showed that the cleavage of the ester bond at peak 1713 cm^{-1} and the formation of the carboxylic acid at peak 1685 cm^{-1} were significantly influenced by UV radiation. Furthermore, the formation of carboxylic acid was considerably higher at saturated humidity and 50 °C conditions compared with dry conditions. The ester bond cleavage was also more pronounced in saturated humidity conditions. The novelty of this study is to provide insights into the chemical degradation of PET under environmental conditions, including UV radiation, humidity, and temperature. The results can be used to develop strategies to reduce the environmental impact of plastic pollution.

Keywords: chemical change; degradation; Fourier transform infrared spectrometry (FTIR); NIST SPHERE; microplastics (MPs); polyethylene terephthalate (PET)



Citation: Rostampour, S.; Cook, R.; Jhang, S.-S.; Li, Y.; Fan, C.; Sung, L.-P. Changes in the Chemical Composition of Polyethylene Terephthalate Under UV Radiation in Various Environmental Conditions. *Polymers* **2024**, *16*, 2249. <https://doi.org/10.3390/polym16162249>

Academic Editor: Shinichi Sakurai

Received: 25 June 2024

Revised: 29 July 2024

Accepted: 31 July 2024

Published: 8 August 2024



Copyright: © 2024 by the authors. Licensee MDPI, Basel, Switzerland. This article is an open access article distributed under the terms and conditions of the Creative Commons Attribution (CC BY) license (<https://creativecommons.org/licenses/by/4.0/>).

1. Introduction

Microplastics (MPs) are emerging contaminants that have been detected in various environments, and significant concerns have been raised over their potentially harmful effects on ecosystems and human health [1–3]. As one of the most widely used synthetic plastics globally, polyethylene terephthalate (PET) has been commonly used in many industries and consumer products due to its low cost, lightweight nature, durability, and high transparency [4–7]. PET ranks fourth among commonly used packaging plastics, raising concerns about the overall plastic footprint and potential environmental impact [8]. Some of the significant applications of PET include plastic bottles and containers, synthetic textile fibers, food and beverage packaging, electronics, automotive parts, and more [6,9–12]. The versatility of PET has led to massive production volumes, with an estimated annual usage of over 30 million tons worldwide [13].

PET's increasing popularity has been accompanied by a surge in plastic pollution, posing a potential environmental and human health threat. Weathering and degradation of PET can release microplastic particles (less than 5 mm) and associated chemical contaminants

into ecosystems, as documented in several studies [14–17]. The long-term consequences of chronic exposure to these microplastics and chemical additives from degraded PET remain largely unknown. For instance, one study estimated that rivers transport between 88 and 95 percent of microplastics to ocean estuaries [18]. PET microplastics have been detected across terrestrial and marine habitats, leading to ingestion and bioaccumulation through the food chain [19–24]. In addition, studies have suggested that ingesting or accumulating these PET degradation microplastics may cause inflammatory, carcinogenic, mutagenic, or endocrine-disrupting effects in organisms [25,26]. PET's degradation can lead to the release of its constituent monomers, such as terephthalic acid, ethylene glycol, and other additive chemicals that have raised toxicological concerns [16,27]. Understanding the environmental degradation pathways of PET is crucial to assessing such ecosystem and human health risks.

PET is a semi-crystalline polyester formed by the polymerization of ethylene glycol and terephthalic acid [28] and can persist in the environment for hundreds of years due to its high resistance to degradation [29,30]. It is well established that solar ultraviolet (UV) radiation facilitates the fragmentation of plastic litter in land and aquatic environments [31,32]. Prior studies have examined the photodegradation of PET under UV radiation and characterized the resulting chemical changes. Radiation with UV-B wavelengths (280 nm to 315 nm) has been found to cause the highest degree of PET degradation [33–35]. The primary photochemical reactions include chain scission of the ester bonds in the PET backbone, leading to reduced molecular weight and oxidation, forming carbonyl and carboxyl groups [36–39]. The ester carbonyl stretching vibration in the PET backbone structure appears at a wavenumber at approximately 1713 cm^{-1} in the mid-range Fourier transform infrared spectroscopy (FTIR) spectrum [40–42]. The intensity of this peak at 1713 cm^{-1} can be used to track the extent of ester bond cleavage during UV exposure. A declining intensity of the absorbance band at 1713 cm^{-1} indicates that the PET polymer chains are undergoing scission at the ester linkages due to photochemical reactions [42,43]. Also, the formation of carboxylic acid photoproducts from PET degradation appears as a peak at approximately 1685 cm^{-1} in the mid-range FTIR spectra. An increase in the intensity of the absorbance band at this wavelength indicates the formation of carbonyl-containing degradation products, which can be used to track the extent of photo-oxidative PET degradation during UV exposure [40,42,44,45]. Previous research has primarily investigated the effects of individual factors, such as hydrothermal degradation, ultraviolet (UV) radiation, or gamma radiation, on the degradation of polyethylene (PE) and polyethylene terephthalate (PET).

Several studies have investigated the impact of temperature on PET degradation, reporting that elevated temperatures above the PET glass transition temperature enhanced photodegradation by increasing chain mobility and oxygen diffusion [15,31,46]. Higher humidity accelerates PET photodegradation through increased moisture penetration and oxidation [47]. It has been established that humidity can induce oxidative processes within the PET aromatic ring, generating volatile degradation compounds [48]. Furthermore, the effects of humidity on different plastic materials are complex and depend on other factors, such as temperature and UV radiation [48]. The degree of UV exposure also directly controls the extent of bond scission and photo-oxidation reactions. The intensity and wavelength of UV radiation can affect the rate of degradation, leading to changes in color and gloss loss for several types of plastic materials [15,49–51]. Research findings have shown that UV radiation affects the speed at which degradation occurs. Nevertheless, the influence of UV radiation on weathering processes can be complex and often interacts with other factors such as temperature and humidity. Most previous photodegradation studies of PET or other plastic materials have focused on limited exposure conditions (e.g., a single temperature or humidity), which leaves gaps in our understanding of how these environmental factors interact to influence the chemical changes in PET under UV radiation.

The unique aspect of this study lies in its systematic investigation of how ultraviolet radiation, humidity, and temperature interact to influence the chemical composition of

polyethylene terephthalate (PET) under controlled conditions replicating real-world environments. In contrast, previous studies have typically focused on the isolated effects of individual factors, such as UV radiation dosage, humidity percentage, or temperature variations, on PET degradation. FTIR detected the PET chemical functional group changes during UV radiation. The studies' results offer valuable information on how PET degrades under different environmental conditions. These findings can help develop effective strategies to reduce the environmental impact of plastic pollution, which is essential for mitigating its ecological risks.

2. Method and Materials

2.1. Sample Preparation

PET samples were prepared from common brands of water bottles. The bottles' upper flat parts (just below the cap) were cut into four samples, each 3 cm to 4 cm in length and 2 cm to 3 cm in width. Before UV exposure, the PET samples were washed with ethanol (Sigma-Aldrich, 100%, St. Louis, MO, USA) to remove surface contaminants. The PET samples were weighed with an analytical balance (METTER TOLEDO model, AB265-S/FACT, Columbus, OH, USA), and their thickness was also measured with a caliper (SPI/13-610-1 model) from ten different locations of the specimen to reach an average thickness. No change in the mass (average = 0.24 g, $n = 60$), standard deviation (SD) = 0.03, and thickness of samples (average = 0.19 mm, $n = 60$, SD = 0.03) was observed after the experiment. After the pre-processing, PET samples were inserted into the photochemical internal environment (PIE) cell for a UV exposure experiment. This is the first time this device has been used for this type of experiment. The PIE cell (Figure 1) is a specialized chamber that studies photochemical reactions under controlled environmental conditions. The PIE cell is made of aluminum (black anodized) with a diameter of 13 cm. Each PIE cell has four chambers sealed by quartz glasses that expose the individual PET samples to different humidity levels. To achieve saturated humidity, deionized water (DI water), provided by NIST, is injected into the cells using a syringe.

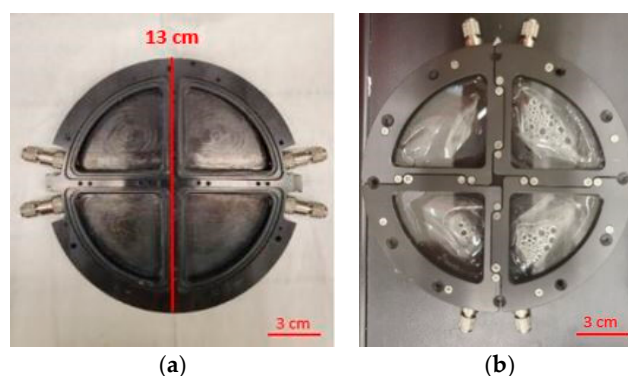


Figure 1. PIE cells (a) without and (b) with samples sealed by glass in a NIST SPHERE chamber under controlled environmental conditions.

2.2. UV Exposures

UV exposure experiments were performed using the NIST-developed SPHERE (simulated photodegradation via high energy radiant exposure) in Gaithersburg, Maryland [48,49]. SPHERE is a 2 m diameter integrating sphere illuminated with six microwave-driven electrodeless metal halide lamps similar to D-type UV curing lamps. The experiment employed a factorial experimental design to investigate the effects of UV intensity, humidity, and temperature on the photodegradation of PET samples. The UV intensity was set at full-intensity UV ($\approx 160 \text{ W/m}^2$, integral intensities from 295 nm to 400 nm, daily dose $\approx 13.8 \text{ MJ/m}^2$) for all experiments [48]. Two levels of humidity were tested: dry conditions (i.e., $\leq 5\%$ relative humidity) and saturated humidity (i.e., $\geq 95\%$ relative humidity). Additionally, the PET samples were exposed to three different temperature levels, 30 °C, 40 °C, and

50 °C, to explore the effects of temperature on PET photodegradation. For each exposure condition, the PET samples were placed in a photochemical internal environment (PIE) sample holder in the SHPERE chambers and exposed to UV radiation for up to 20 days (20 days' exposure in the SPHERE is equivalent to one year of sunlight exposure in South Florida, and 280 MJ/m² in the same spectral range). Samples were removed from the PIE cells every two days after the initial exposure for chemical characterization. This allowed for monitoring chemical changes in the PET samples over the 20-day exposure period.

2.3. Chemical Characterization by Fourier Transform Infrared (FTIR) Spectroscopy Measurements

Chemical changes in the PET samples were characterized via attenuated total reflectance–Fourier transform infrared (ATR-FTIR) spectroscopy (Thermo Scientific, Nicolet iS50, Waltham, MA, USA) [52], similar to methods employed by [53–57]. FTIR has often been used to quantify the carbonyl content in oxidized polymers, using both transmission and ATR techniques to establish oxidation extent and reaction kinetics for degradation comparisons and modeling [58]. Before ATR-FTIR measurements, the sample was placed onto the ATR crystal and pressed down using a swivel press to ensure optimal contact between the sample and the crystal. The measurements were carried out at least three locations for the inner (unexposed) and outer (exposed) surfaces, respectively, of the PET samples. Due to the limited space of the PIE cell, two replicas were used for each exposure time point at various exposure conditions. To gain a better estimate of measurement uncertainty in FTIR-ATR, a series of parallel experiments was conducted using ten PET samples in the same exposure conditions using regular sample holders, as mentioned in [49]. The spectral range was set from 400 cm⁻¹ to 4000 cm⁻¹ with a measurement depth of approximately 2 mm using a diamond ATR crystal. The FTIR spectrum of PET was characterized by specific bands corresponding to various functional groups; this is further discussed in the section on data analysis. After baseline correction, all spectra were normalized to the least-changed band at 1410 cm⁻¹ to minimize the effect of surface morphological changes on the ATR probe-sample contact. The surface became rougher after increased degradation. This peak (1410 cm⁻¹) corresponded to the in-plane aromatic ring deformation vibration in PET. The aromatic rings in PET are relatively stable functional groups and are less likely to undergo significant changes during degradation processes compared with other functional groups in the molecule [37,43,59].

3. Data Analysis

The absorbance level of sensitive bands, such as ester bonds, changes during the degradation process, while the absorbance level of insensitive bands remains constant throughout environmental aging. Therefore, an insensitive band should be used to normalize the absorbance of the sensitive band, as it does not exhibit any tendencies with aging time. The band at a wavelength of 1410 cm⁻¹, attributed to the in-plane ring mode, is unaffected (insensitive) by environmental factors [9,37,43,44,60]. Thus, it is an excellent reference for normalizing spectral intensities among polymers. Variations in IR absorption bands were used to monitor the cleavage of ester groups in the main chain at wavenumber 1713 cm⁻¹, representing carbonyl C=O stretching and being one of the most prominent absorption peaks in FTIR spectra [21,37,42]. Additionally, the formation of carboxyl groups was detected in polymers at the wavenumber of 1685 cm⁻¹, indicating the presence of CO, CO₂, and -COOH (carboxylic acid end groups), which are the primary photodegradation products in PET [35,43,44,61].

The final IR spectra were exported from Omnic software, version 9.12.1002 (Thermo Scientific, Waltham, MA, USA) and imported into Origin Software, version 9.7.0.188 (Origin Lab Corporation, Northampton, MA, USA) for baseline correction to facilitate qualitative analysis. Subsequently, the spectra were normalized at the peak at 1410 cm⁻¹ to investigate chemical changes of the peaks at 1713 cm⁻¹ (indicative of ester bond cleavage) and 1685 cm⁻¹ (indicating the formation of carboxylic acid) in various environmental conditions over different time periods, ranging from a few days to 20 days. Multiple indices were

calculated from the normalized FTIR spectra using a linear end-to-end baseline. These included the vinyl index (peak area integration from 930 cm^{-1} to 880 cm^{-1}), carbonyl index (integration from 1850 cm^{-1} to 1650 cm^{-1}), and hydroxyl index (integration from 3575 cm^{-1} to 3125 cm^{-1}), among others [49,62]. This area-integrated approach was preferred over the more commonly employed peak intensity approach, as it accounted for the different functional groups contributing to the main bands. Since the carbonyl index (CI) can be a valuable indicator for quantifying the extent of PET degradation over time [42], it was calculated by measuring the absorbance at the peak at 1713 cm^{-1} divided by the absorbance at the peak at 1685 cm^{-1} (ester/acid ratio) for the analysis of hydrolysis characterization (Equation (1)).

$$\text{CI} = \frac{\text{cleavage of ester bond at peak } 1713\text{ cm}^{-1}}{\text{formation of carboxylic acid at peak } 1685\text{ cm}^{-1}} \quad (1)$$

It is important to acknowledge that all measurements have inherent uncertainty. This reflects the limitations of the measuring instrument or process itself. This study's error bars represent one standard deviation (SD). The SD calculated from three measurements on the same sample ($n = 3$) in the PIE cell was $\approx 6.2\%$, and the SD for a set of 10 samples ($n = 30$, with three measurements on each sample) exposed to identical conditions was $\approx 6\%$. The measurement uncertainties reported in this paper were obtained by calculating the SDs from a total of 33 measurements ($n = 33$), and the SD value was approximately 6%. Data points indicate the mean, and the error bars present the standard deviation values ($n = 33$).

Deconvolution

The deconvolution of a composite peak into its components is crucial for understanding various types of spectra, including FTIR. Peak-resolving, a technique that relies on the second derivative, is an effective method for distinguishing and resolving overlapping absorbance [42,46]. This technique is particularly valuable for distinguishing between different carboxylic and ester groups within the carbonyl region, as illustrated in Figure 2. Our study aimed to elucidate the use of deconvolution in resolving the complex carbonyl peak into its constituent carboxylic acids and esters, providing insights into PET degradation mechanisms. This provides more detailed information about the specific types of functional groups formed during PET degradation.

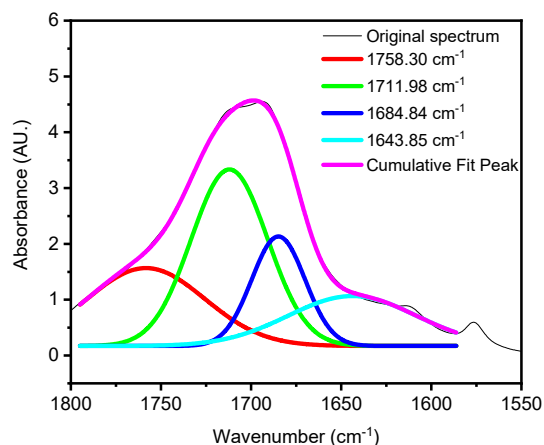


Figure 2. The peak-resolving results in the carbonyl region of PET aged for 20 days at $50\text{ }^{\circ}\text{C}$ in dry conditions.

Figure 2 reveals that the original spectrum comprises four closely situated peaks at (1758 , 1711 , 1684 , and 1643) cm^{-1} . Among these, the peaks at 1685 cm^{-1} and 1643 cm^{-1} may originate from acid-terminated hydrolysis products, while the peaks at 1758 cm^{-1} and 1711 cm^{-1} may represent the absorbance of esters within hydrolysis products in the main chain. The combined areas of the former and latter peaks reflect the total quantity of

acids and esters in the cumulative fitted peaks. In the carbonyl region of an IR spectrum of PET, various carbonyl species overlap, primarily esters and acids derived from terminal carboxyl groups. During the hydrothermal aging of PET, hydrolysis results in the formation of carboxylic and hydroxyl end groups. Consequently, the concentration of carboxylic groups increases with aging time, while that of ester groups decreases. The two peaks at 1711 cm^{-1} and 1758 cm^{-1} can be attributed to the ester group within the main chain, the end carboxyl group, and their hydrogen-bonded associations.

4. Results and Discussion

4.1. Effect of UV Radiation

The chemical properties of PET are essential for specific intended applications, and detecting changes in PET's chemical composition helps us understand its degradation pathway. Initially, PET is ductile and transparent, but it becomes cloudy, yellow, and brittle after degradation [63,64] (Figure 3), while the PET sample in the dry condition is still transparent and soft after 20 days of aging, and there is no noticeable difference in appearance between the dry and untreated samples. These changes result in cracking and surface erosion due to oxidative degradation in the amorphous and crystalline components [65–67]. It is noteworthy that no significant changes in mass or thickness were observed throughout the degradation process.

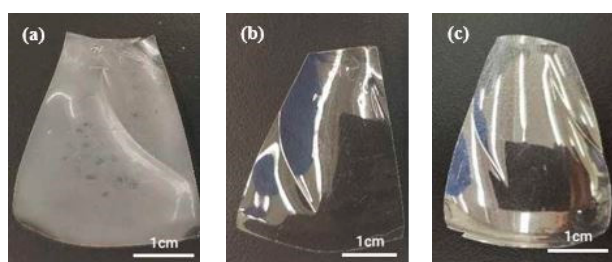


Figure 3. PET samples (a) after 20 days of exposure to $40\text{ }^{\circ}\text{C}$ in saturated humidity, (b) in dry conditions, and (c) before treatment.

Chain scission is one of the primary outcomes of PET photodegradation, leading to increased crystallization and the formation of various degradation products. UV radiation can initiate photo-oxidation reactions, where oxygen reacts with the PET chains, forming new functional groups like peroxides and carboxylic acids. These changes can lead to discoloration, increased surface roughness, and potential leaching of degradation products. In some cases, UV radiation might induce crosslinking reactions between PET chains. This could initially lead to increased rigidity but ultimately contribute to brittleness in the long term. ATR-FTIR was used to identify and quantify surface crystallinity and degradation products, providing a better understanding of how different environmental conditions influence changes in chemical composition. As mentioned in the Section 1, chain scission in PET occurs in the vinyl-ester bond at 1713 cm^{-1} , and one of the degradation products is the confirmation of carboxylic acid at 1685 cm^{-1} [43,68]. The chemical changes are evident on the surface exposed to UV radiation. In contrast, no chemical changes are observed on the inner surface, or the surface not exposed to UV radiation, as illustrated in Figure 4. Nevertheless, other studies have indicated that the mid-range IR spectra of PET bottles' inner and outer surfaces exhibit similar results, suggesting that degradation occurs on both the outside and inside of the bottles under natural marine environment conditions [52,69]. However, the degradation process depends on the life cycle of PET bottles in nature. The most significant cleavage of the ester bond occurs under full-intensity UV radiation, saturated humidity (i.e., $\geq 95\%$ relative humidity), and $50\text{ }^{\circ}\text{C}$ conditions. Figure 4 illustrates a notable distinction between the outer (exposed) and inner (unexposed) surfaces of the PET pieces concerning ester bond cleavage at 1713 cm^{-1} and the presence of carboxylic acid at 1685 cm^{-1} . Understanding UV-induced degradation can inform strategies for PET recycling. Sorting mechanisms could identify and potentially separate highly degraded PET from the

recycling stream to prevent contamination and maintain the quality of recycled materials. Additionally, incorporating UV stabilizers into virgin PET formulations could improve the long-term performance of recycled PET products. The knowledge of how UV radiation affects PET degradation can be integrated into environmental impact assessments. This information can be used to predict the longevity and potential breakdown products of PET litter or microplastics in the environment, aiding in the development of more sustainable materials or waste management strategies.

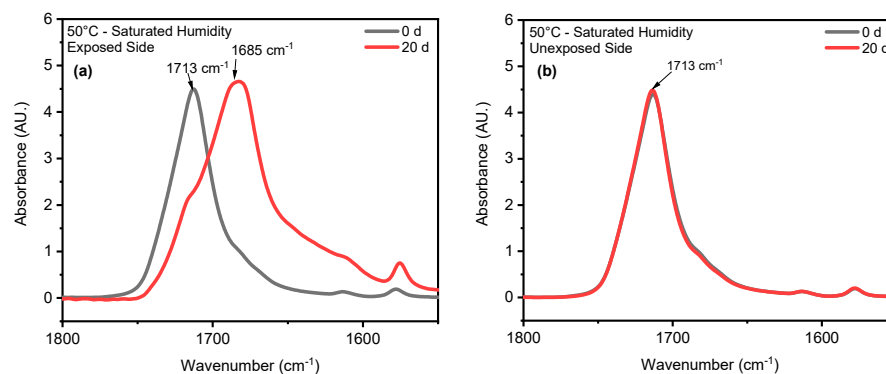


Figure 4. ATR-FTIR results of (a) exposed and (b) unexposed surfaces at 20-day exposure at 50 °C/saturated humidity. The arrows indicate the location 1713 cm^{-1} and 1685 cm^{-1} IR band.

4.2. Effect of Saturated Humidity

The stretching vibrations $-(\text{C}=\text{O})$ of the ester structure in PET are localized at 1713 cm^{-1} and possess different symmetry planes than the aromatic rings, allowing the formation of several structures [62]. As mentioned in the Section 3, the band located at 1410 cm^{-1} , attributed to phenyl ring vibration (C-H bend coupled with ring C-C stretch), serves as a reference band due to its insensitivity to orientation and conformation changes [43,59]. Furthermore, one of the degradation products in PET is the formation of carboxylic acid, evident at a peak of 1685 cm^{-1} [42,44]. Samples were exposed to full radiation under saturated humidity (i.e., $\geq 95\%$ relative humidity) and dry conditions (i.e., $\leq 5\%$ relative humidity) at temperatures of 30 °C, 40 °C, and 50 °C. The results corresponding to Figure 5 demonstrate a decrease in the ester bond at peak 1713 cm^{-1} and an increase in the formation of carboxylic acid at peak 1685 cm^{-1} , similar to other studies [42,43,59,68,70,71]. Also, the results indicated that a saturated humidity (i.e., $\geq 95\%$ relative humidity) environment led to faster degradation at all three temperatures compared with dry conditions (i.e., $\leq 5\%$ relative humidity), attributed to promoting the hydrolysis process in the degradation pathway (Figure 6).

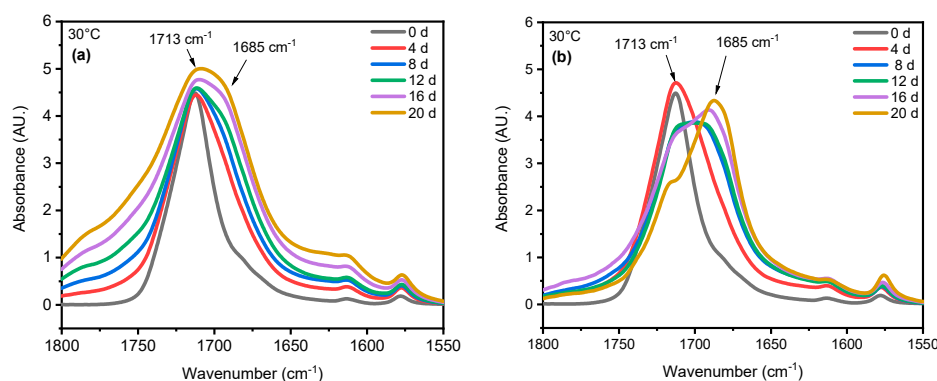


Figure 5. ATR-FTIR results of UV-exposed outer surfaces in (a) dry and (b) saturated humidity conditions at 30 °C. The arrows indicate the location of 1713 cm^{-1} and 1685 cm^{-1} IR bands in the spectrum.

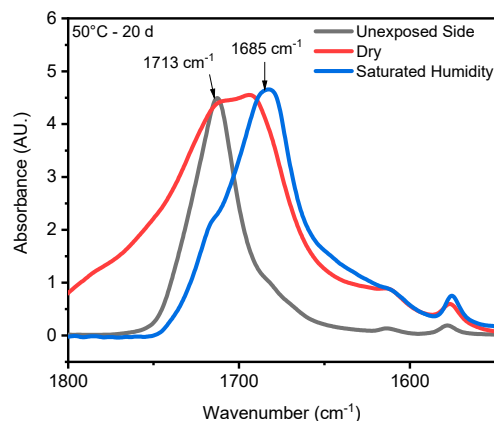


Figure 6. ATR-FTIR results of UV-exposed outer surfaces at 20-day exposure times in both saturated humidity and dry conditions at temperatures of 50 °C. The arrows indicate the location of 1713 cm^{-1} and 1685 cm^{-1} IR bands in the spectrum.

Chain scission occurs when PET is exposed to radiation in the ultraviolet (UV) region and a saturated humidity environment, primarily due to Norrish type I and type II reactions that involve radicals formed in the degradation process. Norrish reactions are a class of photochemical processes involving the light-induced excitation (photoexcitation) of carbonyl-containing molecules ($\text{C}=\text{O}$). Two main types exist: Norrish I reaction leads to the cleavage of the alpha carbon–carbon bond, directly adjacent to the carbonyl group. Depending on the surrounding environment, the resulting fragments may undergo rearrangement within the polymer matrix (polyethylene, PE) to form stable products in their ground state. Norrish II reaction is a more complex reaction involving intramolecular hydrogen atom abstraction. Here, a hydrogen atom from a more distant carbon atom (often the gamma carbon) within the same molecule is transferred to the carbonyl oxygen. This weakens and eventually cleaves the adjacent carbon–carbon bond, ultimately leading to the formation of stable ground-state molecules or inducing a cyclization process (rearrangement) [49,62,68,69,72,73]. The scheme of PET photooxidation is shown in Figure 7 [74]. High-humidity environments promote hydrolysis, a process where water molecules break down the ester linkages within the PET backbone. This reaction yields terephthalic acid (TPA) and ethylene glycol (EG) as primary degradation products, weakening the PET structure and leading to decreased mechanical strength and increased brittleness. While hydrolysis might seem less prevalent in dry conditions, it is important to consider the presence of absorbed water molecules within the PET itself. These internal water molecules can still contribute to hydrolysis over time, albeit at a slower rate compared with saturated environments. Also, the presence of oxygen can exacerbate PET degradation under both humidity conditions. Hydrolysis can create new functional groups like carboxylic acids, which act as sites for free radical attack by oxygen molecules. This initiates oxidative degradation, leading to further chain scission and additional degradation products.

Humidity and UV radiation can have a synergistic effect. UV radiation can initiate chain scission, creating free radicals that further promote oxidative degradation. Additionally, UV radiation might enhance the diffusion of water molecules within the PET structure, potentially accelerating hydrolysis. Our results show that the presence of humidity and full-intensity UV radiation conditions led to an apparent reduction in the ester bond at the peak at 1713 cm^{-1} (Figure 8a). However, this result indicates that ester bond cleavage did not occur under dry UV conditions even with increasing radiation dose, indicating that ester bond cleavage is negligible under dry conditions (Figure 8b). IR spectroscopy is a convenient and concise method for characterizing the degree of hydrolysis, and the ester/acid ratio can serve as a reliable indicator of chain scission in PET, allowing for the quantification of PET degradation. The results illustrate that the decrease at peak 1713 cm^{-1} in saturated humidity conditions was more pronounced than in dry conditions, indicating that humidity plays a significant role in the chain scission of the vinyl–ester bond in the

degradation pathway, regardless of temperature. The carbonyl index also decreased with increasing exposure time, as depicted in Figure 9.

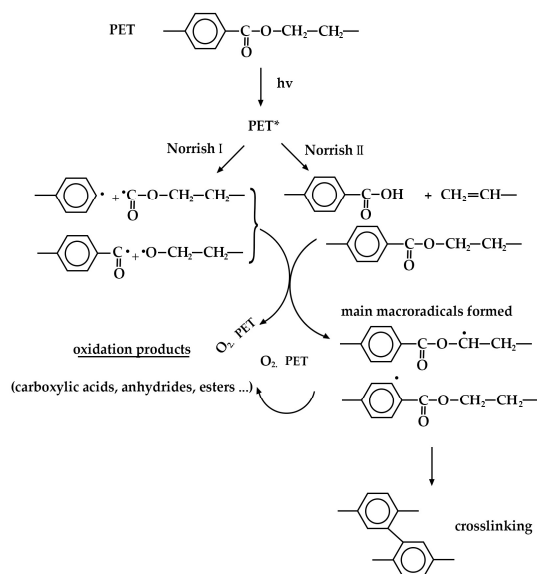


Figure 7. Norrish I and Norrish II reactions in PET.

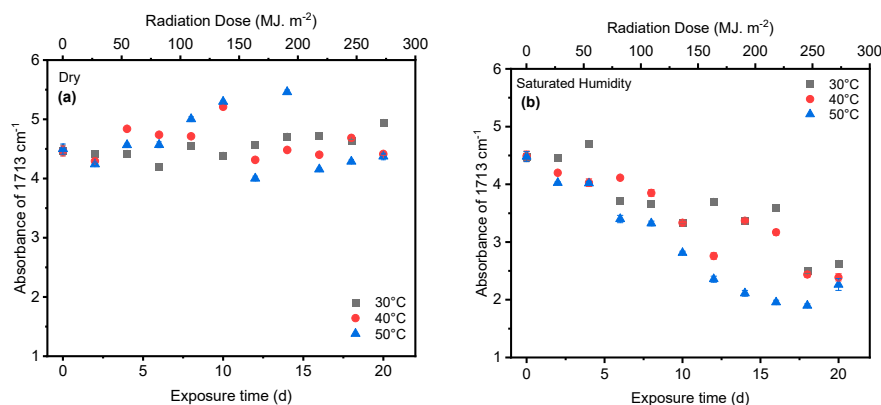


Figure 8. The results of 1713 cm^{-1} cleavage peak in (a) dry and (b) saturated humidity conditions at various temperatures ($30\text{ }^{\circ}\text{C}$, $40\text{ }^{\circ}\text{C}$, and $50\text{ }^{\circ}\text{C}$). Data points indicate the mean, and the error bars present the standard deviation values ($n = 33$).

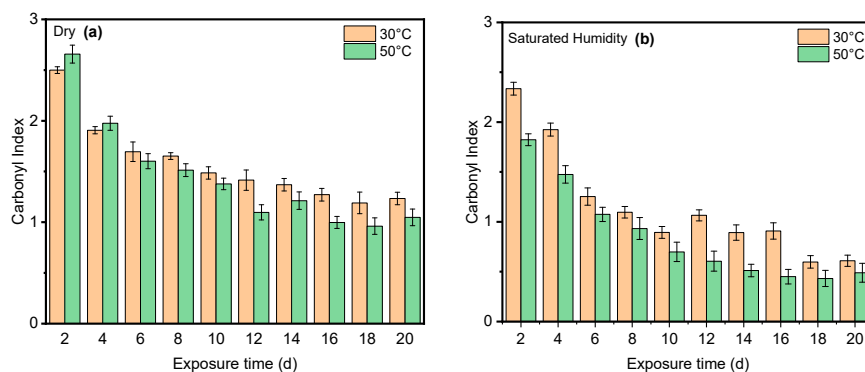


Figure 9. The carbonyl index for PET as a function of exposure time in (a) dry and (b) saturated humidity conditions at $30\text{ }^{\circ}\text{C}$ and $50\text{ }^{\circ}\text{C}$. Data points indicate the mean, and the error bars present the standard deviation values ($n = 33$).

4.3. Effect of Temperature

Temperature is another significant factor influencing the cleavage of the ester bond at the 1713 cm^{-1} peak and the conformation of carboxylic acid at the 1685 cm^{-1} peak. As shown in Figure 10, the carbonyl index at $50\text{ }^{\circ}\text{C}$ was slightly lower than that at $30\text{ }^{\circ}\text{C}$ in both dry and saturated humidity conditions. However, there was no discernible difference in the carbonyl index between $40\text{ }^{\circ}\text{C}$ and $30\text{ }^{\circ}\text{C}$. Moreover, humidity at higher temperatures significantly initiated the degradation of PET compared with dry conditions.

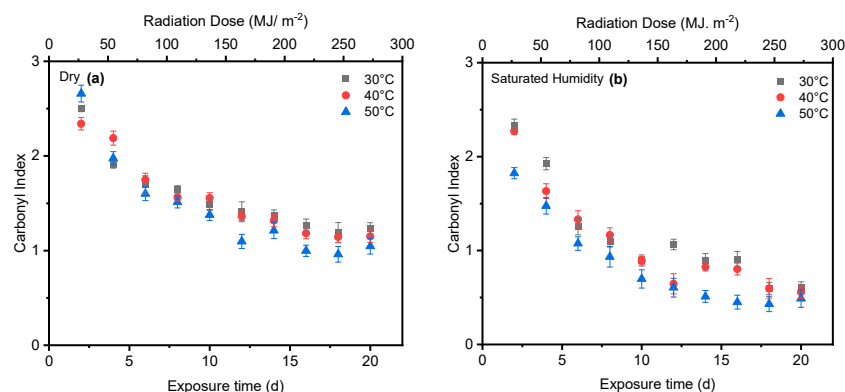


Figure 10. Comparing the cleavage of ester bonds at $30\text{ }^{\circ}\text{C}$, $40\text{ }^{\circ}\text{C}$, and $50\text{ }^{\circ}\text{C}$ under both (a) dry and (b) saturated humidity conditions with the full intensity of UV radiation. Data points indicate the mean, and the error bars present the standard deviation values ($n = 33$).

One study has indicated that, when PET undergoes thermal treatment, its ester bonds break randomly in a process involving a six-membered cyclic transition state. This initial breakdown (pyrolysis) produces vinyl esters and carboxylic acids. These primary products then react further (secondary reactions) to form various byproducts, including carbon monoxide (CO), carbon dioxide (CO_2), acetaldehyde, aromatic acids, and their corresponding vinyl esters [72]. Figure 11 indicates that the formation of a specific chemical compound, carboxylic acid, at peak 1685 cm^{-1} is higher at $50\text{ }^{\circ}\text{C}$ compared with lower temperatures of $30\text{ }^{\circ}\text{C}$ and $40\text{ }^{\circ}\text{C}$. This means that the rate of formation of carboxylic acid produced increases at a higher temperature. Water absorption in PET does increase with temperature, but this alone does not guarantee faster degradation. The rate of PET hydrolysis depends on several factors, including temperature, enzyme concentration, pH, and PET type. While higher temperatures can accelerate hydrolysis [17], the results indicate that a higher temperature ($50\text{ }^{\circ}\text{C}$) initiates the degradation process sooner than a lower temperature ($30\text{ }^{\circ}\text{C}$). Figure 12 shows that, at higher temperatures, the molecules have more kinetic energy, vibrating more intensely and increasing the likelihood of bond breaking. This leads to faster initiation of the degradation process [75,76].

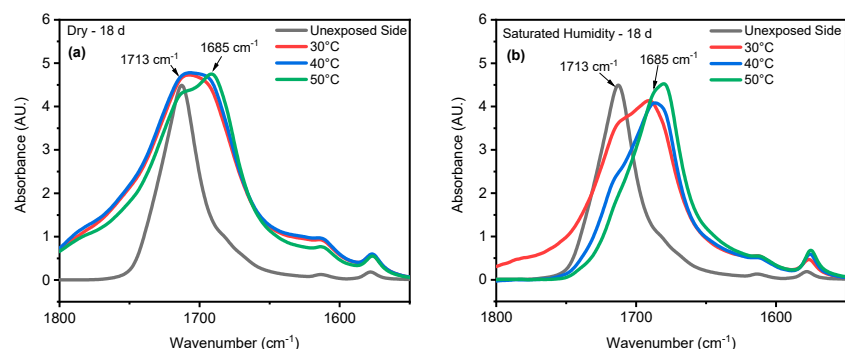


Figure 11. Formation of carboxylic acid at $30\text{ }^{\circ}\text{C}$, $40\text{ }^{\circ}\text{C}$, and $50\text{ }^{\circ}\text{C}$ under both (a) dry and (b) saturated humidity conditions with full-intensity UV radiation after 18 days of exposure time. The arrows indicate the location of 1713 cm^{-1} and 1685 cm^{-1} IR bands in the spectrum.

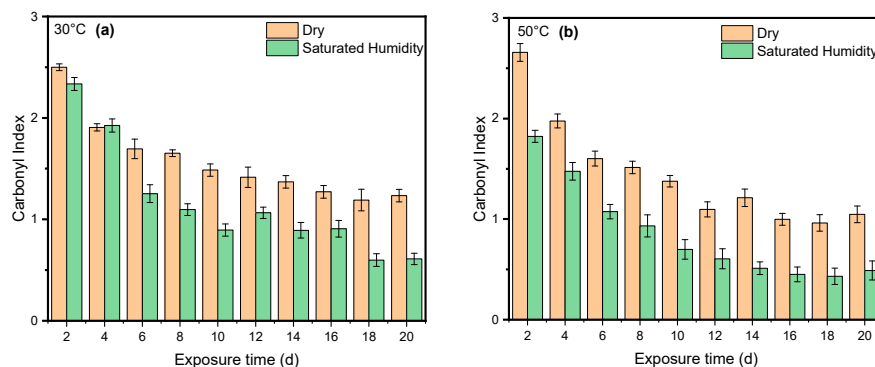


Figure 12. Comparing the cleavage of ester bonds at (a) 30 °C and (b) 50 °C under both dry and saturated humidity conditions with full-intensity UV radiation. Data points indicate the mean, and the error bars present the standard deviation values ($n = 33$).

5. Summary

This study assesses the influence of UV radiation, humidity, and temperature on PET degradation, specifically examining changes in chemical properties and chemical structures. The NIST SPHERE was utilized to accelerate the weathering process under both dry and saturated humidity conditions at temperatures ranging from 30 °C to 50 °C and exposure periods ranging from zero day to 20 days. The data reveal that UV radiation was the most important factor, resulting in the decrease of the ester bond at peak 1713 cm^{-1} and the formation of the carbonyl group at peak 1685 cm^{-1} . However, the unexposed surface of PET pieces displayed no chemical changes, even under conditions of saturated humidity and various temperatures of 30 °C, 40 °C, and 50 °C. The findings indicate that humidity was a key factor in promoting the oxidative breakdown of ester bonds at the 1713 cm^{-1} peak, and this cleavage intensified with increasing exposure times and rising temperatures. Nevertheless, the cleavage of the ester bond at peak 1713 cm^{-1} did not occur in the dry condition at various temperatures. Additionally, the formation of carboxylic acid at the 1685 cm^{-1} peak increased in saturated humidity conditions with higher temperatures and longer exposure times. Therefore, humidity was an essential factor in the breakage of ester bonds in the degradation process. Furthermore, temperature emerged as another factor influencing environmental aging. Results from FTIR indicate increased formation of carboxylic acid at 50 °C compared with 30 °C and 40 °C; this suggests that temperature slightly contributed to the aging process. These conclusions are specific to the tested water bottles and may not necessarily apply to other materials.

Author Contributions: Conceptualization, S.R., C.F., Y.L. and L.-P.S.; methodology, S.R., S.-S.J. and L.-P.S.; software, S.R., R.C. and S.-S.J.; validation, S.R., S.-S.J. and L.-P.S.; formal analysis, S.R., R.C. and S.-S.J.; investigation, S.R. and S.-S.J.; data curation, S.R. and L.-P.S.; writing—original draft, S.R. and C.F.; writing—review and editing, S.R., R.C., Y.L., C.F. and L.-P.S.; supervision, Y.L., C.F. and L.-P.S.; project administration, C.F. and L.-P.S.; funding acquisition, C.F., Y.L. and L.-P.S. All authors have read and agreed to the published version of the manuscript.

Funding: This study was supported by the NIST PREP program with the Johns Hopkins University-Morgan State University HBCU Consortium. Additionally, Chunlei Fan received partial funding from the National Science Foundation (award number 2022887) and the National Institute on Minority Health and Health Disparities of the National Institutes of Health (award number U54MD013376). The content is solely the authors' responsibility and does not necessarily represent the official views of the National Institutes of Health.

Data Availability Statement: The raw/processed data required to reproduce these findings can be shared upon request contingent upon internal approval of the National Institute of Standards and Technology.

Acknowledgments: The author (S.R.) is deeply grateful to the Infrastructure Materials Group at NIST for the invaluable opportunity to access their facilities. The support provided by the NIST Circular

Economy Program and the NIST PREP Program was instrumental to this work. Special thanks are extended to Deborah Jacobs and Karissa Jensen for their dedicated maintenance of the NIST SPHERE during the weathering experiments.

Conflicts of Interest: The authors assert that they have no known competing financial interests or personal relationships that could be perceived as influencing the work reported in this paper.

NIST Disclaimer: Specific commercial products or equipment are described in this paper to adequately specify the experimental procedure. In no case does such identification imply recommendation or endorsement by the National Institute of Standards and Technology, nor does it mean using the best available for the purpose is necessary.

References

1. Seeley, M.E.; Song, B.; Passie, R.; Hale, R.C. Microplastics affect sedimentary microbial communities and nitrogen cycling. *Nat. Commun.* **2020**, *11*, 2372. [[CrossRef](#)]
2. Prata, J.C.; da Costa, J.P.; Lopes, I.; Duarte, A.C.; Rocha-Santos, T. Environmental exposure to microplastics: An overview on possible human health effects. *Sci. Total Environ.* **2020**, *702*, 134455. [[CrossRef](#)]
3. Ivar Do Sul, J.A.; Costa, M.F. The present and future of microplastic pollution in the marine environment. *Environ. Pollut.* **2014**, *185*, 352–364. [[CrossRef](#)]
4. Hopewell, J.; Dvorak, R.; Kosior, E. Plastics recycling: Challenges and opportunities. *Philos. Trans. R. Soc. B Biol. Sci.* **2009**, *364*, 2115–2126. [[CrossRef](#)]
5. Singh, A.K.; Bedi, R.; Kaith, B.S. Composite materials based on recycled polyethylene terephthalate and their properties—A comprehensive review. *Compos. Part B Eng.* **2021**, *219*, 108928. [[CrossRef](#)]
6. Nisticò, R. Polyethylene terephthalate (PET) in the packaging industry. *Polym. Test.* **2020**, *90*, 106707. [[CrossRef](#)]
7. Al-Enizi, A.M.; Ahmed, J.; Ubaidullah, M.; Shaikh, S.F.; Ahamad, T.; Naushad, M.; Zheng, G. Utilization of waste polyethylene terephthalate bottles to develop metal-organic frameworks for energy applications: A clean and feasible approach. *J. Clean. Prod.* **2020**, *248*, 119251. [[CrossRef](#)]
8. Llopis, S.F.; Verdejo, E.; Gil-Castell, O.; Ribes-Greus, A. Partial glycolytic depolymerisation of poly(ethylene terephthalate) (PET) in the solid state: Modelling the contribution of time and temperature. *Polym. Degrad. Stab.* **2024**, *221*, 110695. [[CrossRef](#)]
9. Dubelley, F.; Planes, E.; Bas, C.; Pons, E.; Yrieix, B.; Flandin, L. The hygrothermal degradation of PET in laminated multilayer. *Eur. Polym. J.* **2017**, *87*, 1–13. [[CrossRef](#)]
10. Benyathiar, P.; Kumar, P.; Carpenter, G.; Brace, J.; Mishra, D. Polyethylene Terephthalate (PET) Bottle-to-Bottle Recycling for the Beverage Industry: A Review. *Polymers* **2022**, *14*, 2366. [[CrossRef](#)]
11. Bian, X.; Xia, G.; Xin, J.H.; Jiang, S.; Ma, K. Applications of waste polyethylene terephthalate (PET) based nanostructured materials: A review. *Chemosphere* **2024**, *350*, 141076. [[CrossRef](#)] [[PubMed](#)]
12. Ncube, L.K.; Ude, A.U.; Ogunmuyiwa, E.N.; Zulkifli, R.; Beas, I.N. An overview of plasticwaste generation and management in food packaging industries. *Recycling* **2021**, *6*, 12. [[CrossRef](#)]
13. Geyer, R.; Jambeck, J.R.; Law, K.L. Production, use, and fate of all plastics ever made. *Sci. Adv.* **2017**, *3*, e1700782. [[CrossRef](#)] [[PubMed](#)]
14. Mihai, F.C.; Gündogdu, S.; Markley, L.A.; Olivelli, A.; Khan, F.R.; Gwinnett, C.; Gutberlet, J.; Reyna-Bensusan, N.; Llanquileo-Melgarejo, P.; Meidiana, C.; et al. Plastic Pollution, Waste Management Issues, and Circular Economy Opportunities in Rural Communities. *Sustainability* **2022**, *14*, 20. [[CrossRef](#)]
15. Andrady, A.L.; Barnes, P.W.; Bornman, J.F.; Gouin, T.; Madronich, S.; White, C.C.; Zepp, R.G.; Jansen, M.A.K. Oxidation and fragmentation of plastics in a changing environment; from UV-radiation to biological degradation. *Sci. Total Environ.* **2022**, *851*, 158022. [[CrossRef](#)] [[PubMed](#)]
16. Mishra, R.; Chavda, P.; Kumar, R.; Pandit, R.; Joshi, M.; Kumar, M.; Joshi, C. Exploring genetic landscape of low-density polyethylene degradation for sustainable troubleshooting of plastic pollution at landfills. *Sci. Total Environ.* **2024**, *912*, 168882. [[CrossRef](#)] [[PubMed](#)]
17. Kawai, F.; Kawabata, T.; Oda, M. Current knowledge on enzymatic PET degradation and its possible application to waste stream management and other fields. *Appl. Microbiol. Biotechnol.* **2019**, *103*, 4253–4268. [[CrossRef](#)] [[PubMed](#)]
18. Bhatt, S.; Fan, C.; Liu, M.; Wolfe-Bryant, B. Effect of High-Density Polyethylene Microplastics on the Survival and Development of Eastern Oyster (*Crassostrea virginica*) Larvae. *Int. J. Environ. Res. Public Health* **2023**, *20*, 6142. [[CrossRef](#)] [[PubMed](#)]
19. Koelmans, A.A.; Mohamed Nor, N.H.; Hermesen, E.; Kooi, M.; Mintenig, S.M.; De France, J. Microplastics in freshwaters and drinking water: Critical review and assessment of data quality. *Water Res.* **2019**, *155*, 410–422. [[CrossRef](#)]
20. Evode, N.; Qamar, S.A.; Bilal, M.; Barceló, D.; Iqbal, H.M.N. Plastic waste and its management strategies for environmental sustainability. *Case Stud. Chem. Environ. Eng.* **2021**, *4*, 100142. [[CrossRef](#)]
21. El-Dairi, M.; House, R.J. Microplastics in wastewater treatment plants: Detection, occurrence and removal. *Microplast. Seaf. Implic. Hum. Health* **2019**, *152*, 285–287. [[CrossRef](#)]
22. Dikareva, N.; Simon, K.S. Microplastic pollution in streams spanning an urbanisation gradient. *Environ. Pollut.* **2019**, *250*, 292–299. [[CrossRef](#)] [[PubMed](#)]

23. Mai, L.; He, H.; Zeng, E.Y. *Plastic Pollution in Waterways and in the Oceans*; INC: New York, NY, USA, 2022; Volume 2004, ISBN 9780323998758.
24. Kumar, R.; Manna, C.; Padha, S.; Verma, A.; Sharma, P.; Dhar, A.; Ghosh, A.; Bhattacharya, P. Micro(nano)plastics pollution and human health: How plastics can induce carcinogenesis to humans? *Chemosphere* **2022**, *298*, 134267. [[CrossRef](#)]
25. Groh, K.J.; Backhaus, T.; Carney-Almroth, B.; Geueke, B.; Inostroza, P.A.; Lennquist, A.; Leslie, H.A.; Maffini, M.; Slunge, D.; Trasande, L.; et al. Overview of known plastic packaging-associated chemicals and their hazards. *Sci. Total Environ.* **2019**, *651*, 3253–3268. [[CrossRef](#)] [[PubMed](#)]
26. Al Mamun, A.; Prasetya, T.A.E.; Dewi, I.R.; Ahmad, M. Microplastics in human food chains: Food becoming a threat to health safety. *Sci. Total Environ.* **2023**, *858*, 159834. [[CrossRef](#)]
27. Muncke, J. Exposure to endocrine disrupting compounds via the food chain: Is packaging a relevant source? *Sci. Total Environ.* **2009**, *407*, 4549–4559. [[CrossRef](#)] [[PubMed](#)]
28. Thomsen, T.B.; Hunt, C.J.; Meyer, A.S. Influence of substrate crystallinity and glass transition temperature on enzymatic degradation of polyethylene terephthalate (PET). *New Biotechnol.* **2022**, *69*, 28–35. [[CrossRef](#)]
29. O’Brine, T.; Thompson, R.C. Degradation of plastic carrier bags in the marine environment. *Mar. Pollut. Bull.* **2010**, *60*, 2279–2283. [[CrossRef](#)]
30. Liu, Z.; Zhuang, Q.; Zhang, L.; Meng, L.; Fu, X.; Hou, Y. Polystyrene microplastics induced female reproductive toxicity in mice. *J. Hazard. Mater.* **2022**, *424*, 127629. [[CrossRef](#)]
31. Andrady, A.L.; Heikkilä, A.M.; Pandey, K.K.; Bruckman, L.S.; White, C.C.; Zhu, M.; Zhu, L. Effects of UV radiation on natural and synthetic materials. *Photochem. Photobiol. Sci.* **2023**, *22*, 1177–1202. [[CrossRef](#)]
32. Sørensen, L.; Groven, A.S.; Hovsbakken, I.A.; Del Puerto, O.; Krause, D.F.; Sarno, A.; Booth, A.M. UV degradation of natural and synthetic microfibers causes fragmentation and release of polymer degradation products and chemical additives. *Sci. Total Environ.* **2021**, *755*, 143170. [[CrossRef](#)] [[PubMed](#)]
33. Andrady, A.L. *Biodegradation of Plastics: Monitoring what Happens*; Springer: Berlin/Heidelberg, Germany, 1998; pp. 32–40. [[CrossRef](#)]
34. Fotopoulou, K.N.; Karapanagioti, H.K. Surface properties of beached plastics. *Environ. Sci. Pollut. Res.* **2015**, *22*, 11022–11032. [[CrossRef](#)] [[PubMed](#)]
35. Fotopoulou, K.N.; Karapanagioti, H.K. Degradation of Various Plastics in the Environment. *Handb. Environ. Chem.* **2019**, *78*, 71–92. [[CrossRef](#)]
36. Gulmine, J.; Janissek, P.; Heise, H.; Akcelrud, L. Polyethylene characterization by FTIR. *Polym. Test.* **2002**, *21*, 557–563. [[CrossRef](#)]
37. Mendiburu-Valor, E.; Mondragon, G.; González, N.; Kortaberria, G.; Martin, L.; Eceiza, A.; Peña-Rodríguez, C. Valorization of urban and marine PET waste by optimized chemical recycling. *Resour. Conserv. Recycl.* **2022**, *184*, 106413. [[CrossRef](#)]
38. Le, D.K.; Leung, R.I.H.; Er, A.S.R.; Zhang, X.; Tay, X.J.; Thai, Q.B.; Phan-Thien, N.; Duong, H.M. Applications of functionalized polyethylene terephthalate aerogels from plastic bottle waste. *Waste Manag.* **2019**, *100*, 296–305. [[CrossRef](#)] [[PubMed](#)]
39. Zhang, S.; Xu, W.; Du, R.; Zhou, X.; Liu, X.; Xu, S.; Wang, Y.Z. Cosolvent-promoted selective non-aqueous hydrolysis of PET wastes and facile product separation. *Green Chem.* **2022**, *24*, 3284–3292. [[CrossRef](#)]
40. Gulmine, J.V.; Janissek, P.R.; Heise, H.M.; Akcelrud, L. Degradation profile of polyethylene after artificial accelerated weathering. *Polym. Degrad. Stab.* **2003**, *79*, 385–397. [[CrossRef](#)]
41. Ding, L.; Yu, X.; Guo, X.; Zhang, Y.; Ouyang, Z.; Liu, P.; Zhang, C.; Wang, T.; Jia, H.; Zhu, L. The photodegradation processes and mechanisms of polyvinyl chloride and polyethylene terephthalate microplastic in aquatic environments: Important role of clay minerals. *Water Res.* **2022**, *208*, 117879. [[CrossRef](#)]
42. Du, B.; Yang, R.; Xie, X. Investigation of Hydrolysis in Poly (ethylene terephthalate) by FTIR-ATR. *Chin. J. Polym. Sci.* **2014**, *32*, 230–235. [[CrossRef](#)]
43. Persin, Z.; Mohan, T.; Stana-kleinschek, K. Chemical modification and characterization of poly (ethylene terephthalate) surfaces for collagen immobilization. *Cent. Eur. J. Chem.* **2013**, *11*, 1786–1798. [[CrossRef](#)]
44. Prasad, S.G.; De, A.; De, U. Structural and Optical Investigations of Radiation Damage in Transparent PET Polymer Films. *Int. J. Spectrosc.* **2011**, *2011*, 810936. [[CrossRef](#)]
45. Da Costa, J.P.; Nunes, A.R.; Santos, P.S.M.; Girão, A.V.; Duarte, A.C.; Rocha-Santos, T. Degradation of polyethylene microplastics in seawater: Insights into the environmental degradation of polymers. *J. Environ. Sci. Health Part A* **2018**, *53*, 866–875. [[CrossRef](#)] [[PubMed](#)]
46. Falkenstein, P.; Gräsing, D.; Bielytskyi, P.; Zimmermann, W.; Matysik, J.; Wei, R.; Song, C. UV Pretreatment Impairs the Enzymatic Degradation of Polyethylene Terephthalate. *Front. Microbiol.* **2020**, *11*, 689. [[CrossRef](#)] [[PubMed](#)]
47. Pegram, J.E.; Andrady, A.L. Outdoor weathering of selected polymeric materials under marine exposure conditions. *Polym. Degrad. Stab.* **1989**, *26*, 333–345. [[CrossRef](#)]
48. Pickett, J.E.; Kuvshinnikova, O.; Sung, L.P.; Ermi, B.D. Accelerated weathering parameters for some aromatic engineering thermoplastics. *Polym. Degrad. Stab.* **2019**, *166*, 135–144. [[CrossRef](#)] [[PubMed](#)]
49. Fairbrother, A.; Hsueh, H.; Kim, J.H.; Jacobs, D.; Perry, L.; Goodwin, D.; White, C.; Watson, S.; Sung, L. Temperature and light intensity effects on photodegradation of high-density polyethylene. *Polym. Degrad. Stab.* **2019**, *165*, 153–160. [[CrossRef](#)]
50. Subba Reddy, M.; Srinivasulu Reddy, P.; Venkata, G.; And, S.; Venkata Subbaiah, H. Effect of Plastic Pollution on Environment. *J. Chem. Pharm. Sci.* **2014**, *14*, 28–29.

51. Wu, B.; Wu, H.; Xu, S.M.; Wang, Y.Z. Comparative study of the aging degradation behaviors of PET under artificially accelerated and typical marine environment. *Polym. Degrad. Stab.* **2023**, *217*, 110515. [[CrossRef](#)]
52. Ioakeimidis, C.; Fotopoulou, K.N.; Karapanagioti, H.K.; Geraga, M.; Zeri, C. The degradation potential of PET bottles in the marine environment: An ATR-FTIR based approach. *Sci. Rep.* **2016**, *6*, 23501. [[CrossRef](#)]
53. Fan, C.; Huang, Y.Z.; Lin, J.N.; Li, J. Microplastic constituent identification from admixtures by Fourier-transform infrared (FTIR) spectroscopy: The use of polyethylene terephthalate (PET), polyethylene (PE), polypropylene (PP), polyvinyl chloride (PVC) and nylon (NY) as the model constituent. *Environ. Technol. Innov.* **2021**, *23*, 101798. [[CrossRef](#)]
54. Rathore, C.; Saha, M.; Gupta, P.; Kumar, M.; Naik, A.; de Boer, J. Standardization of micro-FTIR methods and applicability for the detection and identification of microplastics in environmental matrices. *Sci. Total Environ.* **2023**, *888*, 164157. [[CrossRef](#)] [[PubMed](#)]
55. Nolasco, M.E.; Lemos, V.A.S.; López, G.; Soares, S.A.; Feitosa, J.P.M.; Araújo, B.S.; Ayala, A.P.; de Azevedo, M.M.F.; Santos, F.E.P.; Cavalcante, R.M. Morphology, Chemical Characterization and Sources of Microplastics in a Coastal City in the Equatorial Zone with Diverse Anthropogenic Activities (Fortaleza city, Brazil). *J. Polym. Environ.* **2022**, *30*, 2862–2874. [[CrossRef](#)]
56. Lee, H.L.; Chiu, C.W.; Lee, T. Engineering terephthalic acid product from recycling of PET bottles waste for downstream operations. *Chem. Eng. J. Adv.* **2021**, *5*, 100079. [[CrossRef](#)]
57. Enyoh, C.E.; Wang, Q. Automated Classification of Undegraded and Aged Polyethylene Terephthalate Microplastics from ATR-FTIR Spectroscopy using Machine Learning Algorithms. *J. Polym. Environ.* **2024**, 1–16. [[CrossRef](#)]
58. Celina, M.C.; Linde, E.; Martinez, E. Carbonyl Identification and Quantification Uncertainties for Oxidative Polymer Degradation. *Polym. Degrad. Stab.* **2021**, *188*, 109550. [[CrossRef](#)]
59. Chen, Z.; Hay, J.N.; Jenkins, M.J. FTIR spectroscopic analysis of poly (ethylene terephthalate) on crystallization. *Eur. Polym. J.* **2012**, *48*, 1586–1610. [[CrossRef](#)]
60. Endo, T.; Reddy, L.; Nishikawa, H.; Kaneko, S.; Nakamura, Y.; Endo, K. Composite Engineering—Direct Bonding of plastic PET Films by Plasma Irradiation. *Procedia Eng.* **2017**, *171*, 88–103. [[CrossRef](#)]
61. Meng, X.; Zhang, J.; Wang, W.; Gonzalez-Gil, G.; Vrouwenvelder, J.S.; Li, Z. Effects of nano- and microplastics on kidney: Physicochemical properties, bioaccumulation, oxidative stress and immunoreaction. *Chemosphere* **2022**, *288*, 132631. [[CrossRef](#)]
62. Tian, R.; Li, K.; Lin, Y.; Lu, C.; Duan, X. Characterization Techniques of Polymer Aging: From Beginning to End. *Chem. Rev.* **2022**, *123*, 3007–3088. [[CrossRef](#)]
63. Gok, A.; Fagerholm, C.L.; French, R.H.; Bruckman, L.S. Temporal evolution and pathway models of poly(ethylene-terephthalate) degradation under multi-factor accelerated weathering exposures. *PLoS ONE* **2019**, *14*, e0212258. [[CrossRef](#)] [[PubMed](#)]
64. Dhaka, V.; Singh, S.; Anil, A.G.; Sunil Kumar Naik, T.S.; Garg, S.; Samuel, J.; Kumar, M.; Ramamurthy, P.C.; Singh, J. Occurrence, toxicity and remediation of polyethylene terephthalate plastics. A review. *Environ. Chem. Lett.* **2022**, *20*, 1777–1800. [[CrossRef](#)] [[PubMed](#)]
65. Yang, X.; Steck, J.; Yang, J.; Wang, Y.; Suo, Z. Degradable Plastics Are Vulnerable to Cracks. *Engineering* **2021**, *7*, 624–629. [[CrossRef](#)]
66. Min, K.; Cuiffi, J.D.; Mathers, R.T. Ranking environmental degradation trends of plastic marine debris based on physical properties and molecular structure. *Nat. Commun.* **2020**, *11*, 727. [[CrossRef](#)] [[PubMed](#)]
67. Kadoma, A.; Jiao, Q.; Vlassak, J.J.; Suo, Z. Hydrolytic crack growth and embrittlement in poly(ethylene terephthalate). *J. Mech. Phys. Solids* **2023**, *176*, 105303. [[CrossRef](#)]
68. Blanco-Gutiérrez, V.; Li, P.; Berzal-Cabetas, R.; Dos santos-García, A.J. Exploring the photocatalytic activity of nanometric magnetite for PET materials degradation under UV light. *J. Solid State Chem.* **2022**, *316*, 123509. [[CrossRef](#)]
69. Sang, T.; Wallis, C.J.; Hill, G.; Britovsek, G.J.P. Polyethylene terephthalate degradation under natural and accelerated weathering conditions. *Eur. Polym. J.* **2020**, *136*, 109873. [[CrossRef](#)]
70. Al-azzawi, F. Degradation Studies on Recycled Polyethylene Terephthalate. Doctoral Dissertation, London Metropolitan University, London, UK, 2015.
71. Nandiyanto, A.B.D.; Oktiani, R.; Ragadhita, R. Indonesian Journal of Science & Technology How to Read and Interpret FTIR Spectroscopy of Organic Material. *Indones. J. Sci. Technol.* **2019**, *4*, 97–118.
72. Fechine, G.J.M.; Rabello, M.S.; Maior, R.M.S.; Catalani, L.H. Surface characterization of photodegraded poly (ethylene terephthalate). The effect of ultraviolet absorbers. *Polymer* **2004**, *45*, 2303–2308. [[CrossRef](#)]
73. Marchetti, B.; Karsili, T.N.V.; Ashfold, M.N.R. Exploring Norrish type I and type II reactions: An ab initio mechanistic study highlighting singlet-state mediated chemistry. *Phys. Chem. Chem. Phys.* **2019**, *21*, 14418–14428. [[CrossRef](#)]
74. Gardette, J.L.; Colin, A.; Trivis, S.; German, S.; Therias, S. Impact of photooxidative degradation on the oxygen permeability of poly(ethyleneterephthalate). *Polym. Degrad. Stab.* **2014**, *103*, 35–41. [[CrossRef](#)]
75. Das, P.; Tiwari, P. Thermal degradation kinetics of plastics and model selection. *Thermochim. Acta* **2017**, *654*, 191–202. [[CrossRef](#)]
76. Al-Salem, S.M. Kinetic studies related to polymer degradation and stability. In *Plastics to Energy*; Elsevier: Amsterdam, The Netherlands, 2018; ISBN 9780128131404.

Disclaimer/Publisher's Note: The statements, opinions and data contained in all publications are solely those of the individual author(s) and contributor(s) and not of MDPI and/or the editor(s). MDPI and/or the editor(s) disclaim responsibility for any injury to people or property resulting from any ideas, methods, instructions or products referred to in the content.